Scientific
Research
Publishing

A Simple Computational Approach for the Texture Analysis of CT Scan Images Using Orthogonal Moments

Nallasivan Gomathinayagam[1], Janakiraman Subbiah[2]

[1]Department of CSE Einstein College of Engineering, Tirunelveli, India
[2]Department of Banking Technology, Pondicherry University, Pondicherry, India
Email: udhayanallasivan@gmail.com, s.jr@rediffmail.com

Abstract

This paper is a study on texture analysis of Computer Tomography (CT) liver images using orthogonal moment features. Orthogonal moments are used as image feature representation in many applications like invariant pattern recognition of images. Orthogonal moments are proposed here for the diagnosis of any abnormalities on the CT images. The objective of the proposed work is to carry out the comparative study of the performance of orthogonal moments like Zernike, Racah and Legendre moments for the detection of abnormal tissue on CT liver images. The Region of Interest (ROI) based segmentation and watershed segmentation are applied to the input image and the features are extracted with the orthogonal moments and analyses are made with the combination of orthogonal moment with segmentation that provides better accuracy while detecting the tumor. This computational model is tested with many inputs and the performance of the orthogonal moments with segmentation for the texture analysis of CT scan images is computed and compared.

Keywords

1. Introduction

A tumor is the solid lesion which is produced by an abnormal cells growth which seems to be like swelling. The body is composed of many cells and each has a special functions. The extra cells form a mass of tissue called a

tumor. In order to detect tumor, some computerized techniques are essential at the moment for easy diagnose. The advancement in the medical imaging technologies like Computer Tomography (CT), Magnetic Resonance Imaging (MRI) and ultrasonography has significantly raised the accuracy in diagnosing any abnormality in human organs [1]. Even though these technologies are utilized, still there should be more statistical analysis to get the accuracy related to performance analysis. In the field of medical diagnosis, orthogonal moment provides a very good contribution due to its better and superior feature representation capability. Tchebichef moment, a discrete orthogonal moment is suitable for the analysis of image stated by Mukundan [2]. Image analysis using the discrete and continuous orthogonal moment along with the applications was discussed [3]-[5]. Teague [6] introduced both Zernike and Legendre moments based on the theory of continuous orthogonal polynomials and had suggested the notion of orthogonal moments to cover the image from moments. Legendre moments, Zernike moments and Racah moment have been widely used in the since past decades. The classification of texture using Zernike moment feature set was proposed by V.S. bharathi *et al.* [7] who proposed the significance test to select the best moment orders to discriminate normal and abnormal tissues in liver images. Racah Moment, one of the discrete orthogonal polynomials was used for the image analysis stated by Hongqing Zhu *et al.* [8]. The idea so generated can be utilized this orthogonal moment for CT scan images. The classification of CT images using texture features and neural network was proposed by Glestos *et al.* [9]. The Zernike polynomials are orthogonal to each other. Zernike moments can represent the properties of an image with no redundancy or overlap information between the moments [10]. Due to these properties, Zernike moments are found suitable in different types of applications. The performance evaluation of various segmentation methods was analysed by Maheswari *et al.* [11].

The sample of discrete orthogonal moments like Zernike moment and Racah moment is taken for computation. The sample of continuous orthogonal moment like Legendre moment is considered for computation. It is a novel approach of stating the performance of orthogonal moments in terms of computing the accuracy for diagnosing the diseases in medical images. The particular combination of segmentation with orthogonal moments provides very good accuracy while detecting the tumor is studied and compared. The following section covers the implementation of orthogonal moments.

2. Materials and Methods

Regular moments have been extensively used as shape features in a variety of applications in image analysis. The regular moment suffer from the case that the basis function is not orthogonal, and certain degree of information redundancy is also possible. Moments with orthogonal basis functions solve this problem. A brief review of the three orthogonal moments implementation considered in this paper is illustrated as follows.

2.1. Legendre Moment

Legendre moments are a class of continuous orthogonal moments. Teague [6] presented the Legendre moments with the Legendre polynomials as kernel functions. The Legendre moments of $(p + q)$ order for a digital image of pixel size $N \times N$, are defined as,

$$L_{pq} = \left[\frac{(2_q + 1)(2_p + 1)}{(N-1)^2} \right] \sum_{x=1}^{N} \sum_{y=1}^{N} P_P(x_i) P_q(y_i) f(x,y) \tag{1}$$

where the functions $P_p(x_i)$ denote the Legendre polynomials of order "p". The x_i and y_j are the normalized pixel coordinates in the range of [−1, 1]. The Legendre polynomial $P_p(x_i)$ of order "p" is defined as,

$$P_p(x_i) = \sum_{k=0}^{p} \frac{1}{2^p} \frac{(-1)^{(p-1)/2}(p+k)! x_i^k}{k! \left(\frac{p+k}{2} \right)! \left(\frac{p-k}{2} \right)!} \tag{2}$$

with $|x_i| \leq 1$ and $(p$ - $k)$ is even.

2.2. Zernike Moment

Zernike [10] introduced a set of complex polynomials which form a complete orthogonal set over the interior of

the unit circle *i.e.* $x^2 + y^2 = 1$. These polynomials are defined as,

$$V_{pq}(x,y) = R_{pq}(x,y) \exp\left[jq \tan^{-1}(y/x) \right] \tag{3}$$

where p is positive integer or zero and q is positive and negative integers subject to constraints $p - |q|$ even and $|q| \le p$ $R_{pq}(x, y)$: radial polynomial defined as,

$$R_{pq}(x,y) = \frac{\sum_{k=0}^{p-|q|/2} -1^k \left(x^2 + y^2\right)^{(p/2)-k} (p-k)!}{k!\left(\dfrac{p+|q|}{2} - k\right)!\left(\dfrac{p+|q|}{2} - k\right)!} \tag{4}$$

Teague [6] proposed the concept of orthogonal moments, based on orthogonal polynomials. Zernike moments of order "p" with repetition "q" for a digital image function $f(x, y)$ are given by,

$$A_{pq} = \left(\frac{p+1}{\pi}\right) \sum_x \sum_y X_i \left[V_{pq}(x,y)\right]^* f(x,y), \ x^2 + y^2 \le 1 \tag{5}$$

the center of the image is taken as origin for computing the Zernike moment and pixel coordinates are mapped in such a way that $(x^2 + y^2) \le 1$. Those pixels falling outside the unit circle are not used in the computation.

2.3. Racah Moment

The $(n + m)$ order Racah moment of an image $f(s, t)$ with size $N \times N$

$$U_{nm} = \sum_{s=a}^{b-1} \sum_{t=a}^{b-1} \hat{u}_n^{(\alpha,\beta)}(s,a,b) \hat{u}_m^{(\alpha,\beta)}(t,a,b) f(s,t), \quad n,m = 0,1,\cdots,L-1 \tag{6}$$

the set of weighted Racah polynomials being defined as

$$\hat{u}_n^{(\alpha,\beta)}(s,a,b) = u_n^{(\alpha,\beta)}(s,a,b) \sqrt{\frac{\rho(s)}{d_n^2}\left[\Delta x\left(s - \frac{1}{2}\right)\right]}, \quad n = 0,1,\cdots,L-1 \tag{7}$$

$$\rho(s) = \frac{\Gamma(a+s+1)\Gamma(s-a+\beta+1)\Gamma(b+\alpha+s+1)}{\Gamma(a-\beta+s+1)\Gamma(s-a+1)\Gamma(b-s)\Gamma(b+s+1)} \tag{8}$$

$$d_n^2 = \frac{\Gamma(\alpha+n+1)\Gamma(\beta+n+1)\Gamma(b-a+\alpha+\beta+n+1)\Gamma(a+b+\alpha+n+1)}{(\alpha+\beta+2n+1)n!(b-a-n-1)!\Gamma(a+b-\beta-n)} \tag{9}$$

$$u_n^{(\alpha,\beta)}(s,a,b) = \frac{1}{n!}(a-b+1)_n (\beta+1)_n (a+b+\alpha+1)_n$$
$$\times {}_4F_3\left(-n, \alpha+\beta+n+1, a-s, a+s+1; \beta+1, a+1-b, a+b\alpha+1\right), \tag{10}$$
$$n = 0,1,\cdots,L-1; \ s = a, a+1,\cdots,b-1;$$

The generalized hyper geometric function ${}_4F_3$ is given by

$${}_4F_3\left(a_1, a_2, a_3, a_4; b_1, b_2, b_3; z\right) = \sum_{k=0}^{\infty} \frac{(a_1)_k (a_2)_k (a_3)_k (a_4)_k}{(b_1)_k (b_1)_k (b_1)_k} \frac{z^k}{k!} \tag{11}$$

and the parameters a, b, α and β are restricted to

$$-1/2 < a < b, \ \alpha > -1, \ -1 < \beta < 2a+1, \ b = a + N.$$

The weighted set of Racah polynomial values can be obtained by implementing Equation (7).

3. Proposed Method

Classification of CT scan images using hepatic lesions were proposed by Glestos *et al.* [9]. The input CT scan image of size 500×500 is taken as input. The block diagram shows the proposed work in **Figure 1**. The quality of the image is enhanced through the pre-processing stage with morphological operation. The ROI based seg-
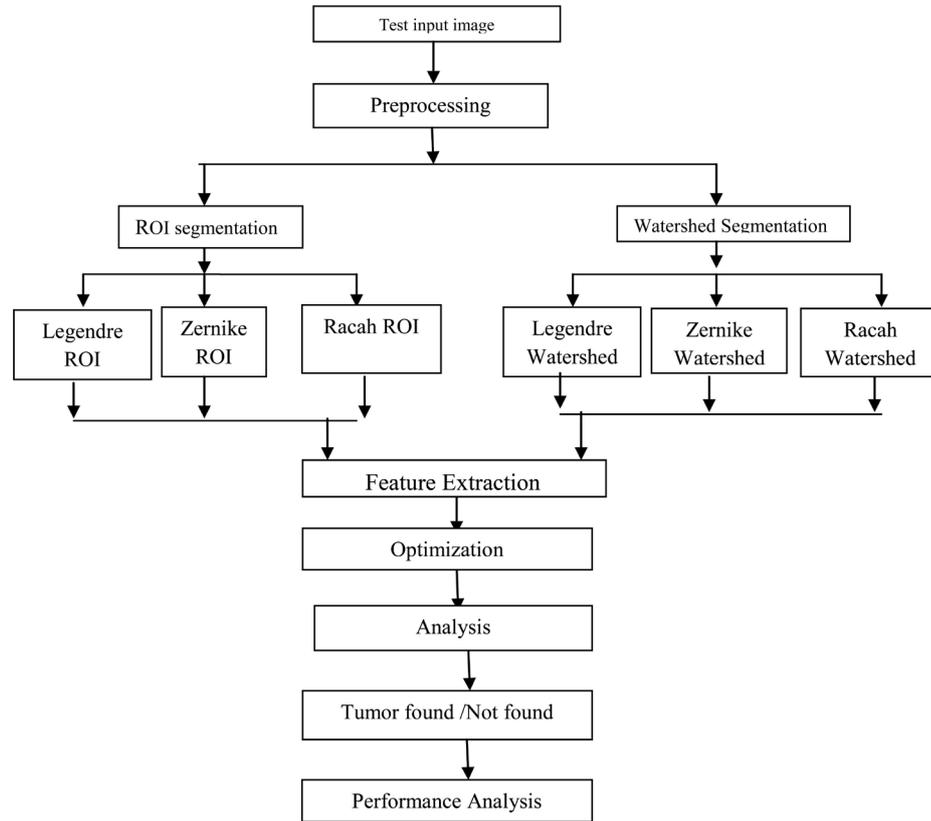
Figure 1. Block diagram of the proposed method.

mentation and Watershed segmentation is applied to the pre-processed image. The two segmented images are applied to the orthogonal moment computation for extracting the features. The discrete and continuous orthogonal moments such as Zernike, Racah and Legendre moments are computed from the ROI and watershed segmented image thereby six different features can be obtained. The mathematical functions like Energy, Contrast, Auto correlation, Homogeneity and variance are computed to extract intensity features of input image. From the six different methods of features, the optimized value is calculated. Based on the optimized values, the threshold is set and using this value the tumor present in the input image is identified. The two segmentation methods output, features are extracted using the Legendre, Zernike and Racah moment so that six different methods can be obtained, applying the following mathematical functions for computing the intensity features.

Energy

$$f_1 = \sum_{i}^{n} \sum_{j}^{n} p(i,j)^2 \tag{12}$$

Contrast

$$f_2 = \sum_{n=0}^{n_g-1} n^2 \left\{ \sum_{i=1}^{N_g} \sum_{j=1}^{N_g} p(i,j) \big\| i-j \big| = n \right\} \tag{13}$$

Auto correlation

$$f_3 = \sum_{i} \sum_{j} (ij) p(i,j) \tag{14}$$

Homogeneity

$$f_4 = \sum_{i} \sum_{j} \frac{1}{1+(i-j)^2} p(i,j) \tag{15}$$

Variance

$$f_5 = \sum_i \sum_j (i - u)^2 \, p(i, j) \tag{16}$$

After computing the above Equations (12)-(16) on the computed orthogonal moments, Energy, autocorrelation, contrast, homogeneity and variance value are obtained for all the input images as in **Table 1**. In order to set the threshold value for detecting the abnormality in the input image, the computed values are optimized for the input images as shown in **Table 2**. As many images are tested with normal and abnormal images, the computational model is performing well enough to detect the tumour. The performance analysis is carried out by using the computed features and the values of each orthogonal moment features are compared with accuracy through sensitivity and specificity.

4. Results and Discussion

The Results of the inputs both normal and abnormal CT scan images which are given as sample inputs and the intermediate outputs are received as presented in the following section.

The sample of input images are used for the experimental study is shown in **Figure 2** and **Figure 3**. The input image is pre-processed and has performed morphological operation to enhance the quality of the input image is given in **Figure 4(a)** and **Figure 4(b)**. The ROI based segmentation and Watershed segmentation is applied on the pre-processed image so as to identify the various regions of the input image is shown in **Figure 4(c)**.

Table 1. Computed intensity features value for the input 2 CT scan image.

	Algorithm	Energy	Contrast	Auto Correlation	Homogeneity	Variance
Input Image 2	Legendre ROI	4.655e−005	21,472.2289	61,518.8844	0.020666	85,160.0753
	Legendre Watershed	4.4531e−006	43,129.4174	63,026.9963	0.021474	84,408.8421
	Zernike ROI	6.5791e−005	22,140.55	62,511.7316	0.0099835	72,536.5954
	Zernike Watershed	−2.8791e−005	20,722.8896	49,470.7831	−0.00083027	30,991.6697
	Racah ROI	4.753e−005	16,584.0676	54,874.0723	0.018438	70,935.5669
	Racah Watershed	2.0716e−005	20,019.3059	64,739.852	0.02322	84,574.3151

Table 2. Optimized value.

Image	Algorithm	Optimized Value
Input Image 2	Legendre ROI	0.13452
	Legendre Watershed	0.15245
	Zernike ROI	0.12575
	Zernike Watershed	0.080948
	Racah ROI	0.11391
	Racah Watershed	0.13547

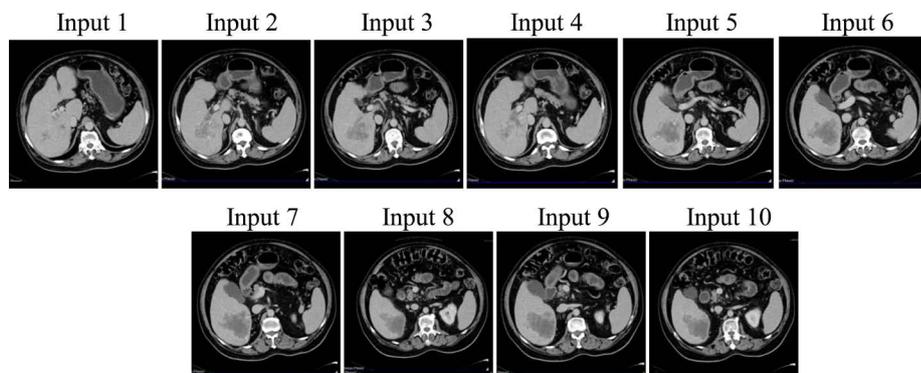**Figure 2.** Sample CT scan input images with abnormalities present.
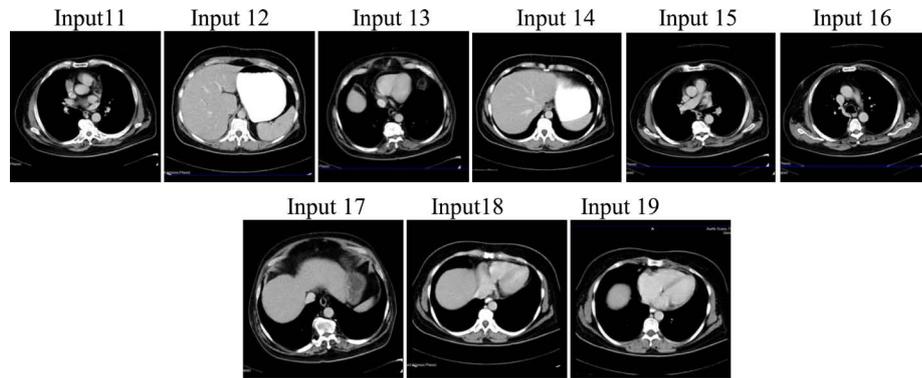
Figure 3. Sample Normal CT scan input images.

(a)   (b)   (c)
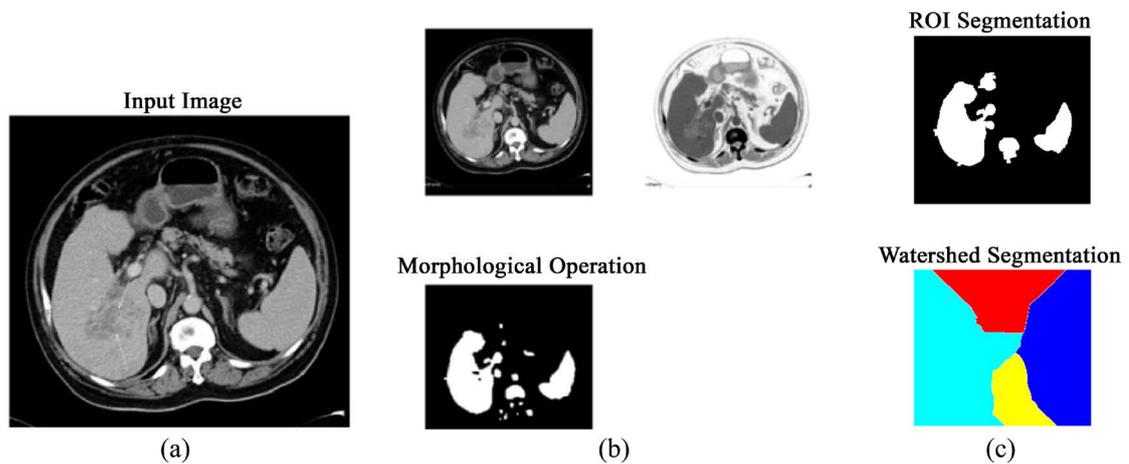
Figure 4. (a) Input 2 CT scan image; (b) Pre-processed Morphological operation on (a); (c) ROI based segmentation and Watershed segmentation output.

Then the three orthogonal moments viz Legendre, Zernike and Racah moments are computed on the two segmented outputs. The intensity features are extracted from the obtained computed moments is presented in **Table 1**. **Table 2** shows the computed optimized value from the obtained intensity features. The Authentication of the input image and the graph representing the computed intensity features are shown in **Figure 5(a)** and **Figure 5(b)**. Similarly the same method is continued for all the input images.

5. Discussion

The various intensity features are extracted from the CT scan input images using Energy, Contrast, Auto correlation etc as shown in **Table 1** and **Table 2**. The computed optimized values for the 19 sample input images with and without tumour is presented below in **Table 3**.

As with many inputs are given and tested, the threshold values have been set as 0.110 by absorbing the Legendre ROI optimized value. Similarly it is possible to set the threshold values for all the six methods. The graph show the analysis of intensity features extracted using the mathematical function like Energy, Contrast, Auto correlation, Homogeneity and variance when compared with six different methods for the sample input images are shown in **Figure 5(b)**.

6. Performance Analysis

The accuracy are calculated based on the parameter of true positive, true negative, false positive, false negative, sensitivity, specificity and positive prediction value and negative prediction value are shown in **Table 4**. The calculations are carried out for all the 19 images, the sample two values for the input image 1 and 2 is presented for the references.
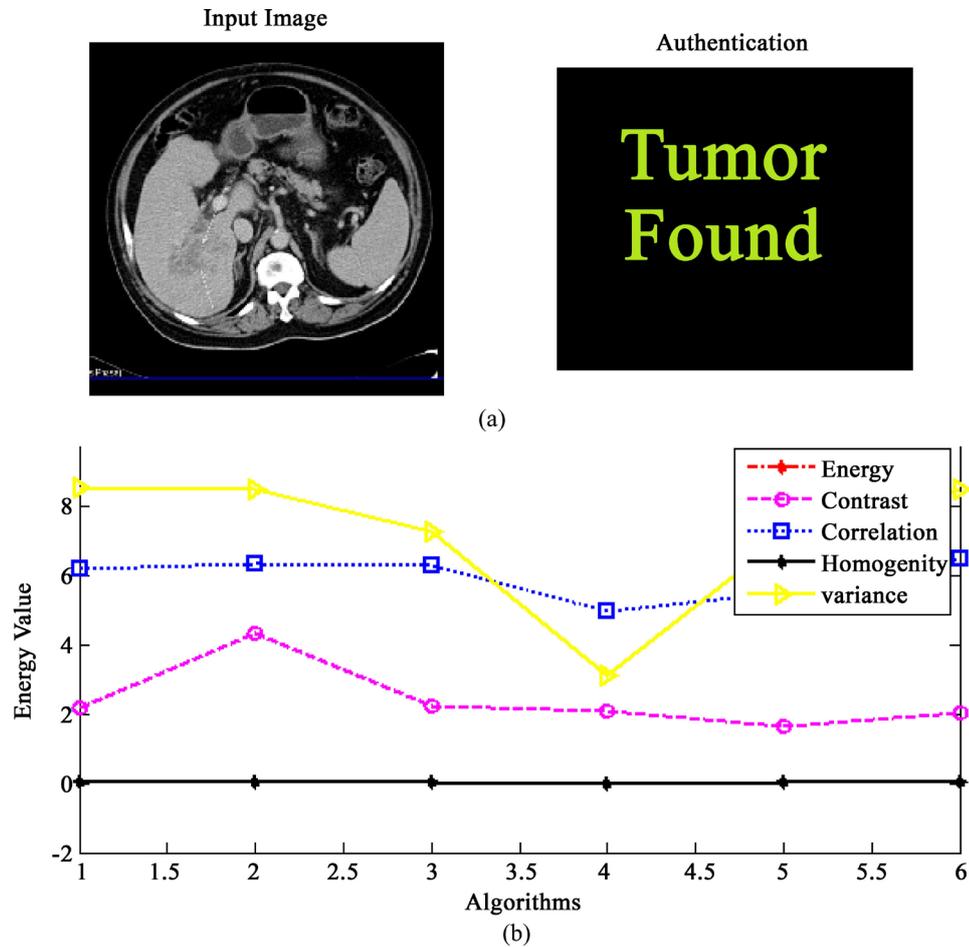
(a)

(b)

Figure 5. (a) Authentication of input image; (b) Graph showing feature extraction computation for the input image 2.

Table 3. Optimized value for the sample input images.

Image Name	Legendre ROI	Legendre Watershed	Zernike ROI	Zernike Watershed	Racah ROI	Racah Watershed	Liver Tumor
Input Image 1	0.11975	0.1491	0.11223	0.069421	0.13413	0.13274	Found
Input Image 2	0.13452	0.15245	0.12575	0.080948	0.11391	0.13547	Found
Input Image 3	0.13182	0.1499	0.12182	0.080992	0.13737	0.13817	Found
Input Image 4	0.12448	0.14935	0.11045	0.075662	0.13713	0.1355	Found
Input Image 5	0.14015	0.15099	0.12063	0.080489	0.13581	0.14079	Found
Input Image 6	0.13708	0.15085	0.1224	0.07299	0.13771	0.14317	Found
Input Image 7	0.16802	0.15498	0.13078	0.089357	0.11243	0.13927	Found
Input Image 8	0.1254	0.14961	0.11156	0.1073	0.15042	0.14001	Found
Input Image 9	0.1433	0.1521	0.13266	0.079602	0.12572	0.14137	Found
Input Image 10	0.13327	0.14945	0.084317	0.080179	0.15242	0.14702	Found
Input Image 11	0.13268	0.15062	0.17135	0.077297	0.13399	0.13255	Not Found
Input Image 12	0.10327	0.15523	0.064337	0.1193	0.11847	0.11513	Not Found
Input Image 13	0.084486	0.15024	0.046296	0.15804	0.089116	0.11707	Not Found
Input Image 14	0.099032	0.15136	0.046378	0.1005	0.10478	0.10881	Not Found
Input Image 15	0.093409	0.15032	0.070749	−0.25465	0.11739	0.13646	Not Found
Input Image 16	0.082372	0.14984	0.21157	0.04008	0.16208	0.14963	Not Found
Input Image 17	0.091154	0.15001	0.091762	−0.095406	0.10255	0.11613	Not Found
Input Image 18	0.085922	0.15027	−0.4817	0.29364	0.10172	0.10492	Not Found
Input Image 19	0.099113	0.14974	0.18833	0.12873	0.13063	0.13001	Not Found

Table 4. Performance analysis of six methods for the sample input images.

	ALGORITHM	TP	TN	FP	FN	Accuracy	Sensitivity	Specificity	PPV	NPV
Input Image 1	Legendre ROI	46.933	49.217	3.066	0.782	96.151	0.9836	0.94135	0.93867	0.98435
	Zernike ROI	43.988	48.466	6.011	1.533	92.454	0.96631	0.88965	0.87977	0.96932
	Racah ROI	47.430	49.344	2.569	0.655	96.775	0.98637	0.95051	0.94861	0.98689
	Legendre WS	44.357	48.103	5.643	1.896	92.460	0.95899	0.89501	0.88714	0.96206
	Zernike WS	20.652	40.134	29.347	9.865	60.787	0.67674	0.57762	0.41304	0.8027
	Racah WS	39.489	46.467	10.510	3.533	85.956	0.91788	0.81553	0.78979	0.92934
Input Image 2	Legendre ROI	45.844	48.967	4.156	1.032	94.811	0.97798	0.92177	0.91688	0.97935
	Zernike ROI	49.374	49.844	0.6254	0.155	99.219	0.99686	0.98761	0.98749	0.99689
	Racah ROI	45.860	48.971	4.139	1.028	94.832	0.97807	0.92206	0.91721	0.97943
	Legendre WS	46.428	48.827	3.571	1.172	95.255	0.97536	0.93184	0.92857	0.97654
	Zernike WS	24.652	41.676	25.347	8.323	66.329	0.74759	.062181	0.49305	0.83354
	Racah Watershed	41.255	47.128	8.744	2.871	88.384	0.93493	0.84349	0.82511	0.94257

Based on the results, it is observed that the Racah polynomial feature extraction for ROI based segmentation provides better accuracy in many input images for 1, 3, 4, 5, 6, 8, 10, 11, 12, 13, 14, 15, 16, 17 and 18. Second to the contribution is Legendre feature extraction for ROI based segmentation and watershed segmentation are placed in terms of accuracy in most of the images. This analysis aids the medical industry to accurately detect tumour and to follow the best orthogonal moment features and segmentation methods.

7. Conclusion

Based on the results, it is observed that the orthogonal moments both discrete and continuous are showing a better feature extraction even in medical images too. The Racah orthogonal moment with ROI based segmentation is showing a very good result in terms of accuracy when compared with other orthogonal moments for the medical images. Followed to this is Legendre moment with ROI based segmentation that shows the better results in accuracy for many images. In order to detect the abnormality present in any CT scan images, the orthogonal moments show very good features representation particularly when combined with ROI based segmentation when compared with other segmentation. Finally, the Racah moment and Legendre moment provide a good contribution when working with Medical images and hence aid the medical field to diagnose the diseases easily. In order to improve the accuracy for diagnosing the diseases in medical images, the proposed work reveals the solution and in future other moments with segmentation can be taken for the study.

References

[1] Subbiah Bharathi, V. and Ganesan, L. (2008) Orthogonal Moments Based Texture Analysis of CT Liver Images. *Pattern Recognition Letters*, **29**, 1868-1872. http://dx.doi.org/10.1016/j.patrec.2008.06.003

[2] Mukundan, R. (2001) Image Analysis by Tchebichef Moments. *IEEE Transactions On Image Processing*, **10**, 1357-1365. http://dx.doi.org/10.1109/83.941859

[3] Mukundan, R., Ong, S.H. and Lee, P.A. (1980) Discrete vs. Continuous Orthogonal Moments for Image Analysis. Faculty of Information Science and Technology, Multimedia University, Malaysia.

[4] Shen, J., Shen, W., Shen, D.F. and Wu, Y.F. (2004) Orthogonal Moments and Their Application to Motion Detection in Image Sequences. *International Journal of Information Acquisition*, **1**, 77-87. http://dx.doi.org/10.1142/S0219878904000045

[5] Torres-Méndez, L.A., Ruiz-Suárez, J.C., Sucar, L.E. and Gómez, G. (2000) Translation, Rotation, and Scale-Invariant Object Recognition. *IEEE Transactions on Systems*, *Man*, *and Cybernetics—Part C*: *Applications and Reviews*, **30**, 125-130.

[6] Teague, M.R. (1980) Image Analysis via the General Theory of Moments. *Journal of the Optical Society of America*, **70**, 920-930. http://dx.doi.org/10.1364/JOSA.70.000920

[7] Bharathi, V.S., Raghavan, V.S. and Ganesan, L. (2002) Texture Classification Using Zernike Moments. *The 2nd FAE*

International Symposium, European University of Lefke, Turkey, 1 October 2008, 292-294.

[8] Zhu, H.Q., *et al.* (2006) Image Analysis by Discrete Orthogonal Racah Moments. *Signal Processing*, **87**, 687-708. http://dx.doi.org/10.1016/j.sigpro.2006.07.007

[9] Glestos, M., Mougiakakou, S.G., Matsopoulos, G.K., Nikita, K.S., Nikita, A.S. and Kelekis, D. (2001) Classification of Hepatic Lesions from CT Images Using Texture Features and Neural Networks. *Proceedings of* 23*rd Annual EMBS International Conference*, Turkey, 2748-2752.

[10] Von Zernike, F. (1934) Beugungstheorie des schneidenver-fahrens und seiner verbesserten form, der phasenkontrast-methode. *Physica*, **1**, 689-704. http://dx.doi.org/10.1016/S0031-8914(34)80259-5

[11] Mageswari, S.U. (2014) Analysis and Performance Evaluation of Various Image Segmentation Methods. *International Conference on Contemporary Computing and Informatics* (*IC*3*I*), Mysore, 27-29 November 2014, 469-474. http://dx.doi.org/10.1109/ic3i.2014.7019614